Radioprotection
© The Authors, published by EDP Sciences 2023
https://doi.org/10.1051/radiopro/2023009

Available online at:
www.radioprotection.org

ARTICLE OPEN ACCESS

Effect of new radioprotective equipment on reducing radiation exposure of participants in percutaneous coronary intervention

F. Liu[1,2,3,*], Raja[3,4], Z. You[2], J. Wang[5], W. Li[1], Y. Wu[1], W. Suthakorn[3] and L. Liao[2]

[1] Cardiac Interventional Imaging Center, The First Affiliated Hospital, Hengyang Medical School, University of South China, 421001, Hengyang City, Hunan Province, People's Republic of China.
[2] School of Nursing, University of South China, Hengyang City, Hunan Province, People's Republic of China.
[3] PhD Degree Program, Faculty of Nursing, Chiang Mai University, Chiang Mai, Thailand.
[4] Department of Plastic and Reconstructive Surgery, Dr. Ruth K.M. Pfau Civil Hospital, Karachi, Pakistan.
[5] Occupational Health Department, Hengyang Traditional Chinese Medicine Hospital, Hunan, People's Republic of China.

Received: 15 November 2022 / Accepted: 27 February 2023

Abstract – Background: The ionising radiation generated in percutaneous coronary intervention has the largest hazard to medical staff among all interventional procedures, and thus has gained the attention of various researchers. Radioprotective shielding equipment is an effective measure; however, it has poor applicability to diverse interventional procedures. The aim of this study was to develop a new radioprotective shielding equipment for percutaneous coronary intervention and determine its effectiveness and applicability. **Methods:** This study developed a radioprotective cabin for percutaneous coronary intervention and used fluoroscopy and cine models of a digital subtraction angiography machine to compare the effectiveness of experimental (radioprotective cabin) and control (current radioprotection strategies) groups. Radiation equivalent dose rates were measured at 231 data points: 210 points were distributed on four vertical planes around the therapy bed and 21 points were evenly distributed around the thyroid, head, and gonad areas of a standardised patient. **Results:** Based on the cine model, there were statistically significant differences in the radiation equivalent dose rates between the control and experimental groups in the left plane, right plane, foot plane, head area, and gonad area ($Z = -6.645$, -5.615, -6.204, -2.647, -2.882, respectively; $P < 0.05$). Based on the fluoroscopy model, there were statistically significant differences in the radiation equivalent dose rates between the two groups in the left plane, right plane, foot plane, and gonad area ($Z = -6.060$, -5.083, -5.203, -2.887, respectively; $P < 0.05$). **Conclusion:** The radioprotective cabin developed in this study can effectively reduce the radiation equivalent dose rates in the standing area of medical staff and radiation-sensitive areas of patients without affecting the operation, which can be promoted and applied in percutaneous coronary intervention.

Keywords: coronary interventional procedure / radioprotective cabin / radioprotection / occupational safety / patient safety

1 Introduction

Coronary heart disease (CHD) is a serious health threat owing to its high morbidity, mortality, recurrence, and complications (Mensah *et al.*, 2019). Percutaneous coronary intervention (PCI) has become one of the preferred treatments for CHD owing to its minimally invasive nature, short hospitalisation period, and significant healing effect. The number of PCI procedures has significantly increased annually, with the number of PCI cases in China reaching more than 1,164,117 in 2021.

PCI requires the operator to use X-rays to guide the intervention, which is associated with high levels of ionising radiation exposure (Behan *et al.*, 2010). In addition, prolonged radiation exposure increases the risk of radiation illnesses (Rajaraman *et al.*, 2016; Roguin *et al.*, 2013; Uwineza *et al.*, 2019), including diseases such as tumours and immune disorders (Kreuzer *et al.*, 2018). A study on interventional radioprotection in Argentina found lens opacities in 91% of physicians, 77% of technicians, and 100% of nurses (Papp *et al.*, 2017). The international recommendation for radiation exposure should be average 20 mSv per year within five years, and not exceed 50 mSv in any year (D'Avino *et al.*, 2019). However, a substantial proportion of interventional medical staff are exposed to radiation beyond this dose limit (Domienik *et al.*, 2016).

*Corresponding author: wind1022@163.com

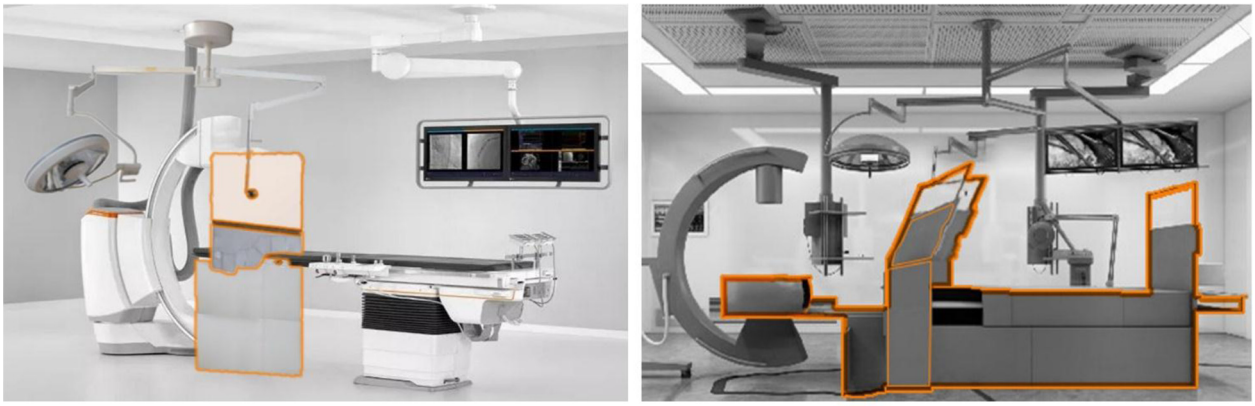

A: Current radioprotection strategies B: New Radioprotective Cabin

Fig. 1. Overview of current radioprotection strategies and new radioprotective cabin.

In the PCI procedure, physicians need to manually control the guiding catheters and wires, change the angle of the digital subtraction angiography (DSA) machine beam tube constantly, stay closer to the bed, and cannot shorten the X-ray emission time to observe the guiding wires and catheters more clearly (Monzen *et al.*, 2017). In addition, physicians and nurses focus on the procedure and rarely pay attention to the radiation equivalent dose rate (EDR), which is used to assess the strength of radiation (Bera *et al.*, 2018); thus, medical staff in this procedure are often exposed to more radiation than in other interventional procedures (Madder *et al.*, 2018), and the patients are entirely exposed to radiation. Therefore, this study focused on designing and investigating better and stricter shielding radioprotective equipment to reduce intraoperative radiation hazards in PCI and safeguard the lives of physicians, nurses, and patients.

2 Methods

2.1 Material settings

2.1.1 DSA machine radioprotective cabin design

This experiment was carried out using a radioprotective cabin (Fig. 1B), which was compared with current radioprotection strategies (Fig. 1A). The radioprotective cabin developed by the first author has obtained a patent. It had a compartment for patients, fabricated using lead plates, that can accommodate the patient who will be protected up and down by the lead material, except for the patient's heart area. The patient compartment, composed of lead plates, comprised three sub-covers, which were nested sequentially according to different sizes, and the staff could easily fold the patient compartment when the patient gets on and off the bed. There were movable baffles in the middle and tail of the safety cabin. The bottom of the middle baffle was installed on the upper side of the safety cabin and its top was suspended from the room ceiling. Furthermore, the tail baffle was equipped with an infusion pump, defibrillator, and medicine cabinet. The radioprotective cabin was designed with an operation area, a guiding wire and catheter placement slot, infusion, and contrast media connection holes. Moreover, a head shield was designed at the location of the patient's head to protect it from radiation, and three lead curtains were set around the bed. All the above-mentioned components were fabricated using lead materials, such as lead glass, lead sheets, and lead plates.

2.1.2 DSA machine, data acquisition dot matrices, and standardised patient settings

2.1.2.1 DSA machine settings

A DSA machine (Artis Zee III floor, Siemens) equipped with a therapy bed with a length of 300 cm and a width of 90 cm was used in the experiment. The beam tube of the DSA machine was in the posterior-anterior position, the cine model was Card 2020, and the fluoroscopy model was FL Card, with image acquisition frames of 7.5, 15, and 30 f/s. The acquisition field of view was set at 20 cm × 20 cm, the bed was the lowest point at −23 cm, the X-ray receiver plate was set at the lowest level, and the X-ray beam tube was 90 cm from the X-ray receiving plate. The bed was moved so that the central position of the heart, where the steel ball was located, was in the centre of the field of view. The cine and fluoroscopy pedals were used to initiate the coronary angiography and fluoroscopy-guided operations.

2.1.2.2 Radiation acquisition dot matrix settings

Radiation alert inspector radiation detector made in the USA was used as a radiation monitor. Radiation EDR was measured at 231 data points: 210 were distributed on the four vertical planes around the therapy bed and 21 were evenly distributed around the standardised patient's thyroid, head, and gonadal areas. Based on the length and width of the bed and medical staff's forearm length (30 cm), maximum height (180 cm), and general standing location, four vertical detection planes were set 30 cm away from the bed using a wooden frame, as shown in Figure 2A. x1 and y1, x2 and y2, x3 and y3, and x4 and y4 formed four radiation EDR data acquisition dot matrices. The width and height of the vertical radiation detection planes on the left and right sides of the bed were 300 and 180 cm, respectively, and the width and height of the vertical radiation detection planes on the cephalad and foot sides of the bed were 90 and 180 cm, respectively. Three radiation EDR data acquisition dot matrices were set in patient's head, thyroid, and gonad areas; the locations of the dots are shown in Figure 2B.

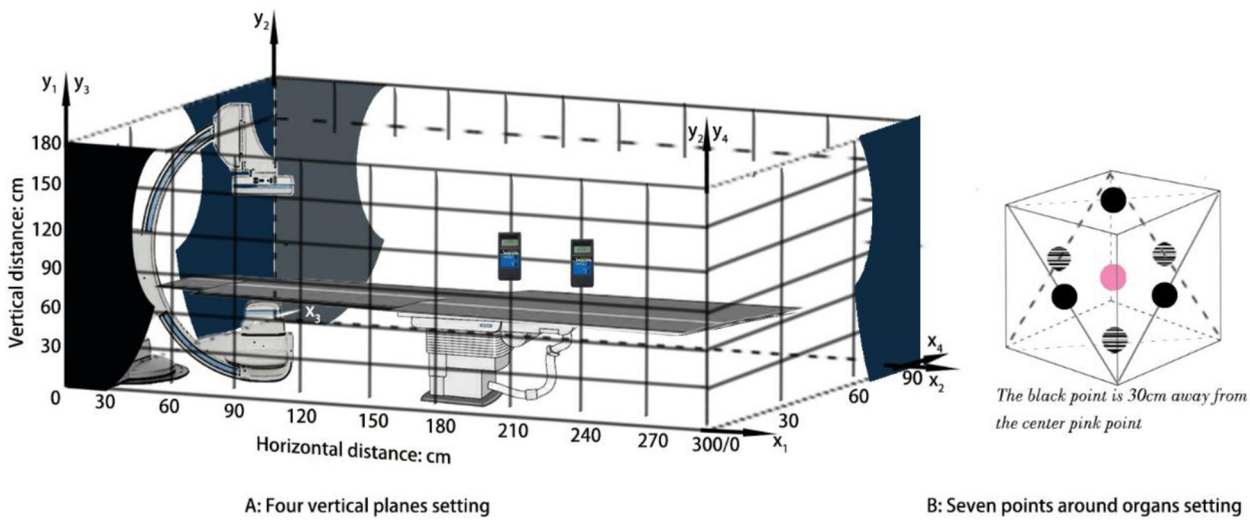

Fig. 2. Acquisition dot matrixes of radiation equivalent dose rate.

2.1.2.3 Standardised patient settings

A standardised patient, made of plexiglass of uniform material, was used as the patient model. It was fabricated with the bilateral shoulder positions, left and right anterior axillary line positions, and heart location marked on the model. The model was placed horizontally on the bed to simulate patients' normal chest and abdominal position during PCI.

2.2 Research methods

2.2.1 Measurement methods

The DSA machine parameters were kept unchanged, and the intersection of the cephalad of the bed unit and the floor level was set to zero on the left and right sides, as shown in Figure 2A. The Y-axis values (cm) of 0, 30, 60, 90, 120, 150, and 180 were indicated on the left and right vertical detection planes of the bed unit formed by the wooden frame. The horizontal X-axis values (cm) corresponding to each vertical Y-axis value were adjusted to 0, 30, 60, 90, 120, 150, 180, 210, 240, 270, and 300. The radiation detector was placed at each intersection of X- and Y-axes values, and the ray acquisition window faced the bed unit. One hundred and fifty-four radiation EDR data were collected, corresponding to two vertical detection planes.

Another two vertical radiation detection planes were constructed using a wooden frame. The intersection of the right side of the bed unit and the floor level was set to zero on the cephalad and foot sides, as shown in Figure 2A. The Y-axis values (cm) of 0, 30, 60, 90, 120, 150, and 180 were indicated on the cephalad and foot vertical detection planes of the bed unit formed by the wooden frame. The horizontal X-axis values (cm) corresponding to each vertical Y-axis value were adjusted to 0, 30, 60, and 90. The radiation detector was placed at each intersection of X- and Y-axes values, and the ray acquisition window faced the bed unit. Fifty-six radiation EDR data points were collected, corresponding to two vertical detection planes.

Other radiation EDR points were set around patients' head, thyroid, and gonadal areas. Seven different radiation detection points were established to collect radiation EDR data, including the central point of radiation-sensitive organs and six points 30 cm away from the centre of each sensitive organ in six directions, as shown in Figure 2B. Twenty-one radiation EDR data points were collected, corresponding to three radiation acquisition dot matrices of each sensitive organ.

The radiation EDR data were measured for a single ray emission time of 60 s, and the final stable radiation EDR value within 60 s was observed, recorded, and plotted. Standardised patient model made of plexiglass was used, and the surveyors were all outside the room when the radiation was beamed.

2.2.2 Allocation

This study developed a radioprotective cabin for PCI and used fluoroscopy and cine models of a DSA machine, respectively, to compare the effectiveness of radioprotection between the control group (current radioprotection strategies) and experimental group (radioprotective cabin). Current radioprotection strategies use hanging lead screen and lead curtain at the bedside, which routinely droop without folds and gaps, and the lower edge is close to the bed unit surface, as shown in Figure 1A. The experimental group utilised a radioprotective cabin without a bedside lead curtain and hanging lead screen, as shown in Figure 1B. A total of 231 radiation EDR data using fluoroscopy model and 231 using cine model were obtained from each group. Finally, 924 radiation EDR data points were collected for this study. This study was approved by the institutional review board.

2.2.3 Statistical methods

The data were processed using SPSS 17.0, and the Kolmogorov-Smirnov test showed that none of the data conformed to a normal distribution; therefore, median and inter-quartile range (IQR) were used as statistical descriptors. The Mann-Whitney U test was used to compare the two groups, which satisfied the sample size requirement. A P-value < 0.05 was considered statistically significant.

Table 1. Effectiveness and rationality of radiation qcquisition spacing setting (Sv/h).

Groups	Cases	FPS 7.5 p/s		FPS 15 p/s		FPS 30 p/s	
		Median	IQR	Median	IQR	Median	IQR
$X=0$ cm	7	24.10	6.26	48.07	7.30	98.11	32.05
$X=30$ cm	7	28.77	5.15	58.54	13.81	120.3	29.80
$X=60$ cm	7	30.78	4.65	60.17	14.08	127.9	27.50
$X=90$ cm	7	23.97	3.57	49.25	10.75	103	24.60
$X=120$ cm	7	16.86	4.75	33.99	12.40	64.59	17.16
$X=150$ cm	7	9.65	6.22	16.63	5.57	38.54	20.46
$X=180$ cm	7	4.65	4.80	8.65	6.71	18.82	15.2
$X=210$ cm	7	2.04	1.4	5.31	3.84	8.75	7.77
$X=240$ cm	7	1.06	1.08	1.93	1.18	5.88	6.60
$X=270$ cm	7	0.53	0.48	1.10	0.81	2.95	2.54
$X=300$ cm	7	0.65	0.35	1.01	0.60	3.28	2.90
H		72.296	71.220	71.429			
P		0.001*	0.001*	0.001*			

IQR: inter-quartile range.
* $P<0.05$.

3 Results

3.1 Analysis of the effectiveness and rationality of radiation acquisition spacing setting

The detection points corresponding to the vertical Y-axis were divided into 11 groups based on the different detection points on the horizontal X-axis, and the results are listed in Table 1. Table 1 shows that the differences among the 11 groups of data were statistically significant when the same image acquisition frames ($H=72.296$, 71.220, 71.429; $P<0.05$) were compared. A 30-cm radiation acquisition spacing was found effective and rational.

3.2 EDR analysis between the two groups in the same cine model acquisition matrix

The radiation EDR data of the two groups from the cine operations were drawn into radiation EDR distribution maps, as shown in Figure 3, and listed in Table 2. Comparing the radiation EDR data of the two groups, there were statistically significant differences between the control and experimental groups in the left plane, right plane, foot plane, head area, and gonad area ($Z=-6.645$, -5.615, -6.204, -2.647, -2.882, respectively; $P<0.05$), and the radioprotection effectiveness of the experimental group was better than that of the control group. There were no significant differences between the two groups in the cephalad plane and thyroid area ($Z=-0.057$, -0.160, respectively; $P>0.05$).

3.3 EDR analysis between the two groups in the same fluoroscopy model acquisition matrix

The radiation EDR data of the two groups from the fluoroscopy operations were drawn into radiation EDR maps, as shown in Figure 4 and listed in Table 3. Comparing the radiation EDR data of the two groups, there were statistically significant differences between the control and experimental groups in the left plane, right plane, foot plane, and gonad area ($Z=-6.060$, -5.083, -5.203, -2.887, respectively; $P<0.05$), and the radioprotection effectiveness of the experimental group was better than that of the control group. There were no significant differences in the cephalad plane, thyroid, and head area between the two groups ($Z=-0.180$, -0.241, -0.961, $P>0.05$).

4 Discussion

Radioprotection during medical examination and treatment is mainly achieved based on three aspects: time, distance, and shielding protection (Monzen *et al.*, 2017). Currently, DSA machines are equipped with partial non-closed lead curtains on the right side of the bed unit, which reduces radiation exposure for doctors during interventional procedures. However, no radioprotection-shielding equipment is set on the other side of the bed unit, and the radioprotective effectiveness of patients is weaker. When operating on patients with chronic total occlusion (CTO), doctors, nurses, and patients may be exposed to higher radiation doses because the procedure can last longer (Mares and Mukherjee, 2021).

When using the radioprotective cabin, the radiation EDR in the left plane, right plane, foot plane of the bed unit, and patient's gonad area were significantly lower based on the cine and fluoroscopy model than those using current radioprotection strategies. However, the radiation EDR in the cephalad plane of the bed unit and patient's thyroid area were not significantly reduced in the two models compared with using current radioprotection strategies. This may be related to the lack of lead shielding by the radioprotective cabin in these two areas. In the patient's head area, the radiation EDR dropped significantly when the radioprotective cabin was used during the cine operation but not during fluoroscopy, which may be

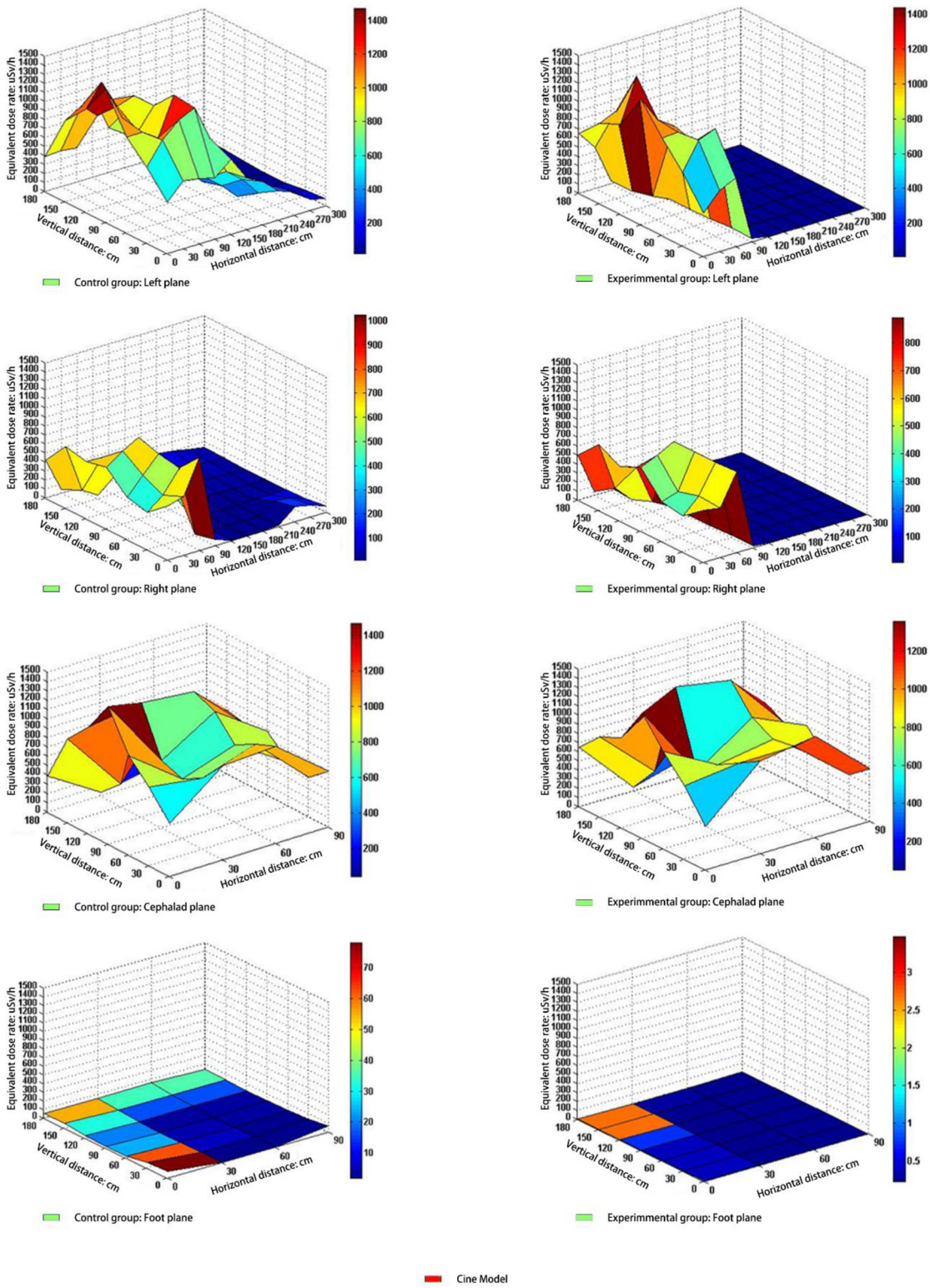

Fig. 3. Radiation EDR distribution maps of cine operation in control and experimental group.

Table 2. Radiation equivalent dose rate analysis of cine operation in 2 groups (Sv/h).

Acquisition matrix	Cases	Control group		Experimental group		Z	P
		Median	IQR	Median	IQR		
Left plane	77	394.00	802.65	6.5	65.91	−6.645	0.001*
Right plane	77	92.30	382.85	4.3	36.90	−5.615	0.001*
Cephalad plane	28	741.00	541.25	770.5	488.5	−0.057	0.954
Foot side plane	28	24.05	43.48	0.38	0.86	−6.204	0.001*
Thyroid area of patient	7	502.00	239.75	462	310.5	−0.160	0.873
Head and face of patient	7	955.50	144.25	535	315.5	−2.647	0.008*
Gonads area of patient	7	1210.0	284.75	2.83	0.91	−2.882	0.004*

IQR: inter-quartile range.
* $P < 0.05$.

related to the low radiation EDR of X-ray emitted by the DSA machine during fluoroscopy, resulting in increased scattering when the X-ray passed through the operating bed and the standardised patient.

The radioprotective cabin developed in this study can effectively reduce the radiation EDR in the doctor's standing area (right plane of the bed unit); its effectiveness is better than that of current radioprotection strategies. It can effectively reduce the radiation EDR in the nurse's standing area (left plane and foot plane). It can effectively reduce the radiation EDR on patient's sensitive glands (gonad). It can protect sensitive organs, such as the eyes and brain.

The PCI procedure is a complex procedure. During the procedure, doctors need to operate the guiding catheter, guiding wire, balloon, contrast agent syringe, and other consumables needed during the operation. Nurses need to perform intravenous infusion, electrical defibrillation, and drug dispensing. In this study, an operation area, guiding wire and catheter placement slot, connection hole for infusion and contrast agent, and connection hole were set up for electrocardiogram monitoring and defibrillation in the radioprotective cabin, which facilitated the operation. Because of the multidirectional changes in the DSA beam tube angle during the coronary interventional procedure, a vertically adjustable movable baffle and movable three-layer chamber were designed. After testing, it did not affect in the changes of the angle of the DSA machine beam tubes during the PCI. This indicates that the design of the radioprotective cabin is reasonable and convenient for clinical applications because it reduces radiation EDR (Etzel *et al.*, 2018; Fattal and Goldstein, 2013).

5 Study limitations

Because the lead products required for the entire production of the radioprotective cabin are expensive, a steel skeleton based on the radioprotective cabin structure was built, and the outer layer was covered by lead sheets with a lead equivalent of 0.5 mm Pb. This model probably caused bias in the experimental data. A single-brand DSA machine and unified standard body model were used in this study. In practice, radiation EDR data may vary with the DSA machine brand and the patient's body size. In future studies, we will continue to improve the radioprotective cabin and apply it in clinics to enhance the representativeness of the results.

6 Conclusion

The radioprotective cabin developed in this study can effectively reduce exposure of interventional doctors, nurses, and patients to radiation during PCI.

Conflict of interest

The authors declare that they have no conflicts of interest in relation to this article.

Funding

Natural Science Foundation of Hunan Province, 2021JJ40489. Scientific research project of Hunan Provincial Health Commission, 202212013945. Hunan Province General Colleges and Universities Teaching Reform Research Fund, HNJG-2021-0635.

Ethical approval

Ethical approval of the study was granted from the First Affiliated Hospital of University of South China.

Informed consent

In this research, standardised patient, made of plexiglass of uniform material, was used as the patient model. Hence, informed consent was not applicable.

Authors' contributions

Fenggang Liu: the conceived idea, designed radioprotective equipment, manuscript writing, figure drafting.

Raja: data analysis and interpretation, manuscript writing.

Ze You: contributed to draft writing, proofreading.

Juanjuan Wang, Wu Li, Yingying Wu: data collection, critical review.

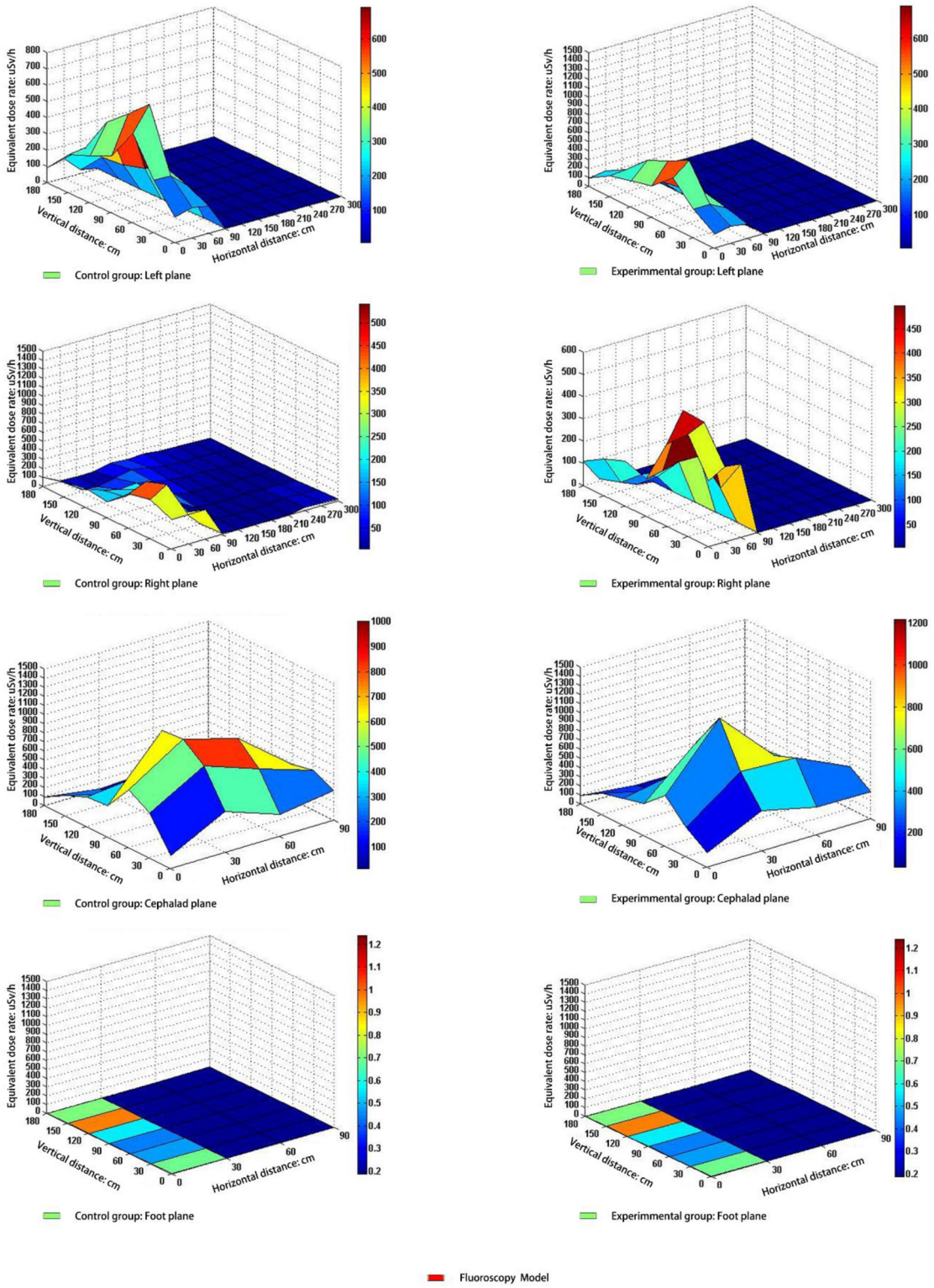

Fig. 4. Radiation EDR distribution maps of fluoroscopy operation in control and experimental group.

Table 3. Radiation equivalent dose rate analysis of fluoroscopy operation in 2 groups (Sv/h).

Acquisition matrix	Cases	Control group		Experimental group		Z	P
		Median	IQR	Median	IQR		
Left plane	77	98.3	194.85	1.3	106.31	−6.060	0.001*
Right plane	77	19.8	86.49	1.03	9.60	−5.083	0.001*
Cephalad plane	28	333	372	310.5	380.5	−0.180	0.857
Foot side plane	28	6.05	11.375	0.2	0.31	−5.203	0.001*
Thyroid area of patient	7	965	148.25	1005	417	−0.241	0.810
Head and face of patient	7	647	288.25	605	281.25	−0.961	0.337
Gonads area of patient	7	308	129.75	0.35	0.17	−2.887	0.004*

IQR: inter-quartile range.
* $P < 0.05$.

Weeraporn Suthakorn and Li Liao: supervised whole process of study.

All authors read and approved the final manuscript.

Acknowledgements

We are highly thankful to the funding organizations to support this study; without their support it was not possible.

References

Behan M, Haworth P, Colley P, Brittain M, Hince A, Clarke M, Ghuran A, Saha M, Hildick-Smith D. 2010. Decreasing operators' radiation exposure during coronary procedures: the transradial radiation protection board. *Catheter. Cardiovasc. Interv.* 76(1): 79–84. https://doi.org/10.1002/ccd.22466.

Bera G, Soret M, Maisonobe J-A, Giron A, Garnier J-M, Habert M-O, Kas A. 2018. Equivalent dose rate from patients after whole-body FDG-PET/CT. *Med. Nucl.* 42(1): 45–48.

D'Avino V, Angrisani L, La Verde G, Pugliese M, Raulo A, Sabatino G, Coppola F. 2019. New eye lens dose limit: status of knowledge in Campania hospitals. *Int. J. Environ. Res. Public Health* 16(18). https://doi.org/10.3390/ijerph16183450.

Domienik J, Bissinger A, Grabowicz W, Jankowski Ł, Kręcki R, Makowski M, Masiarek K, Plewka M, Lubiński A, Peruga JZ. 2016. The impact of various protective tools on the dose reduction in the eye lens in an interventional cardiology-clinical study. *J. Radiol. Prot.* 36(2): 309–318. https://doi.org/10.1088/0952-4746/36/2/309.

Etzel R, König AM, Keil B, Fiebich M, Mahnken AH. 2018. Effectiveness of a new radiation protection system in the interventional radiology setting. *Eur. J. Radiol.* 106: 56–61. https://doi.org/10.1016/j.ejrad.2018.07.006.

Fattal P, Goldstein JA. 2013. A novel complete radiation protection system eliminates physician radiation exposure and leaded aprons. *Catheter. Cardiovasc. Interv.* 82(1): 11–16. https://doi.org/10.1002/ccd.24625.

Kreuzer M, Auvinen A, Cardis E, Durante M, Harms-Ringdahl M, Jourdain JR, Madas BG, Ottolenghi A, Pazzaglia S, Prise KM, Quintens R, Sabatier L, Bouffler S. 2018. Multidisciplinary European Low Dose Initiative (MELODI): strategic research agenda for low dose radiation risk research. *Radiat. Environ. Biophys.* 57(1): 5–15. https://doi.org/10.1007/s00411-017-0726-1.

Madder RD, La Combe A, Van Oosterhout S, Mulder A, Elmore M, Parker JL, Jacoby ME, Wohns D. 2018. Radiation exposure among scrub technologists and nurse circulators during cardiac catheterization: the impact of accessory lead shields. *JACC Cardiovasc. Interv.* 11(2): 206–212. https://doi.org/10.1016/j.jcin.2017.07.026.

Mares A, Mukherjee D. 2021. Management of chronic total occlusion of coronary artery. *Int. J. Angiol.* 30(1): 48–52. https://doi.org/10.1055/s-0040-1721478.

Mensah GA, Roth GA, Fuster V. 2019. The global burden of cardiovascular diseases and risk factors: 2020 and beyond. *J. Am. Coll. Cardiol.* 74(20): 2529–2532. https://doi.org/10.1016/j.jacc.2019.10.009.

Monzen H, Tamura M, Shimomura K, Onishi Y, Nakayama S, Fujimoto T, Matsumoto K, Hanaoka K, Kamomae T. 2017. A novel radiation protection device based on tungsten functional paper for application in interventional radiology. *J. Appl. Clin. Med. Phys.* 18(3): 215–220. https://doi.org/10.1002/acm2.12083.

Papp C, Romano-Miller M, Descalzo A, Michelin S, Molinari A, Rossini A, Plotkin C, Bodino G, Esperanza G, Di Giorgio M, Touzet R. 2017. Results of relid study 2014-Buenos Aires, Argentina retrospective evaluation of lens injuries and dose. *Radiat. Prot. Dosimetry* 173(1–3): 212–217. https://doi.org/10.1093/rpd/ncw339.

Rajaraman P, Doody MM, Yu CL, Preston DL, Miller JS, Sigurdson AJ, Freedman DM, Alexander BH, Little MP, Miller DL, Linet MS. 2016. Cancer risks in U.S. radiologic technologists working with fluoroscopically guided interventional procedures,1994–2008. *AJR Am. J. Roentgenol.* 206(5): 1101–1108 (quiz 1109). https://doi.org/10.2214/ajr.15.15265.

Roguin A, Goldstein J, Bar O, Goldstein JA. 2013. Brain and neck tumors among physicians performing interventional procedures. *Am. J. Cardiol.* 111(9): 1368–1372. https://doi.org/10.1016/j.amjcard.2012.12.060.

Uwineza A, Kalligeraki AA, Hamada N, Jarrin M, Quinlan RA. 2019. Cataractogenic load – A concept to study the contribution of ionizing radiation to accelerated aging in the eye lens. *Mutat. Res. Rev. Mutat. Res.* 779: 68–81. https://doi.org/10.1016/j.mrrev.2019.02.004.

Cite this article as: Liu F, Raja, You Z, Wang J, Li W, Wu Y, Suthakorn W, Liao L. 2023. Effect of new radioprotective equipment on reducing radiation exposure of participants in percutaneous coronary intervention. *Radioprotection* 58(2): 91–98